

<https://doi.org/10.1038/s42003-024-06011-0>

Accelerated nitrogen cycling on Mediterranean seagrass leaves at volcanic CO₂ vents



Johanna Berlinghof^{1,2,3,9}✉, Luis M. Montilla^{1,9}, Friederike Peiffer^{1,2}, Grazia M. Quero⁴, Ugo Marzocchi^{1,5}, Travis B. Meador^{6,7}, Francesca Margiotta⁸, Maria Abagnale⁸, Christian Wild² & Ulisse Cardini^{1,3}✉

Seagrass meadows form highly productive and diverse ecosystems in coastal areas worldwide, where they are increasingly exposed to ocean acidification (OA). Efficient nitrogen (N) cycling and uptake are essential to maintain plant productivity, but the effects of OA on N transformations in these systems are poorly understood. Here we show that complete N cycling occurs on leaves of the Mediterranean seagrass *Posidonia oceanica* at a volcanic CO₂ vent near Ischia Island (Italy), with OA affecting both N gain and loss while the epiphytic microbial community structure remains largely unaffected. Daily leaf-associated N₂ fixation contributes to 35% of the plant's N demand under ambient pH, while it contributes to 45% under OA. Nitrification potential is only detected under OA, and N-loss via N₂ production increases, although the balance remains decisively in favor of enhanced N gain. Our work highlights the role of the N-cycling microbiome in seagrass adaptation to OA, with key N transformations accelerating towards increased N gain.

Seagrass meadows are highly productive ecosystems worldwide, often occurring in nutrient-limited coastal areas¹. They are among the most ecologically and economically valuable ecosystems on Earth². Providing habitat, breeding grounds, and food for a wide range of organisms, they are considered 'hotspots' for biodiversity³. They also play an important role in sequestering large amounts of carbon, comparable to terrestrial forests⁴. In particular, the Mediterranean seagrass *Posidonia oceanica* can contribute to climate change mitigation through its effective CO₂ uptake and large sequestration capacity⁵ and may even act as a buffer against ocean acidification (OA) by temporarily raising the seawater pH through its daylight photosynthesis⁶. This is relevant since the Mediterranean Sea has a higher capacity to absorb anthropogenic CO₂ than other oceans due to its particular CO₂ chemistry and active overturning circulation⁷. The pH of the Mediterranean Sea in the Western basin is predicted to decrease between 0.245 under the most optimistic scenario of the

"Special Report: Emissions Scenarios" (SRES) of the IPCC (2007) and 0.462 units under the most pessimistic SRES scenario⁸.

Generally, marine plants are expected to benefit from increased CO₂ concentrations as their photosynthetic rates are undersaturated at current CO₂ levels⁹. However, OA has multifaceted effects on *P. oceanica*. Photosynthetic performance of *P. oceanica* seedlings and net leaf productivity increase under high pCO₂^{10–12}, while OA has little effect on the net community production of *P. oceanica* but results in increased shoot density and shorter leaf length due to increased herbivory^{12–14}. Calcareous epiphytes such as encrusting red algae, bryozoans, foraminifers, and spirorbids decline or even disappear under OA, while non-calcareous invertebrates such as hydrozoans and tunicates benefit^{12,15–17}.

Much less attention has been paid to the effects of OA on the biogeochemical cycling of elements other than carbon, such as nitrogen (N). Nitrogen is an essential nutrient for all living organisms and can be a limiting factor for primary production in marine seagrasses¹⁸, with its availability

¹Department of Integrative Marine Ecology, Stazione Zoologica Anton Dohrn – National Institute of Marine Biology, Ecology and Biotechnology, Naples, Italy.

²Department of Marine Ecology, University of Bremen, Bremen, Germany. ³Genoa Marine Centre, Stazione Zoologica Anton Dohrn – National Institute of Marine Biology, Ecology and Biotechnology, Genova, Italy. ⁴Institute for Marine Biological Resources and Biotechnology, National Research Council (CNR), Ancona, Italy.

⁵Center for water technology (WATEC), Department of Biology, Aarhus University, Aarhus, Denmark. ⁶Biology Centre of the Czech Academy of Sciences, České Budějovice, Czech Republic. ⁷Department of Ecosystem Biology, Faculty of Science, University of South Bohemia, České Budějovice, Czech Republic.

⁸Department of Research Infrastructures for marine biological resources, Stazione Zoologica Anton Dohrn – National Institute of Marine Biology, Ecology and Biotechnology, Naples, Italy. ⁹These authors contributed equally: Johanna Berlinghof, Luis M. Montilla. ✉ e-mail: johber@uni-bremen.de; ulisse.cardini@szn.it

depending on diverse N transformation processes that are performed by a complex network of metabolically diverse microorganisms¹⁹. Seawater pH affects N speciation and concentration, which in turn affects metabolic processes and N transformations^{20,21}. Dinitrogen (N₂) fixation by N₂-fixing bacteria and archaea (i.e., diazotrophs) has often been found to increase under OA^{21,22}. The reason is not always clear, but in phototrophs, it may involve more energy being redirected to the demanding N₂ fixation process owing to the down-regulation of carbon-concentrating mechanisms^{21,23,24}. Autotrophic microbial nitrification can be highly sensitive to pH, and nitrification in the open ocean has been found to be considerably reduced by OA²⁵. Dissimilatory nitrate reduction processes (e.g., denitrification or anaerobic ammonium oxidation - anammox), which are modular and involve many different bacterial groups often found in low-pH environments, are thought to be less affected by OA, with rates showing contrasting results at low seawater pH²¹.

Many N-cycling microorganisms can be found in close association with *P. oceanica*, together forming a holobiont^{26,27}. Seagrass-associated microbes can enhance the N access via ammonification and genes for microbial ammonification can be found ubiquitously in this system²⁸. N₂ fixation by associated diazotrophic microorganisms can be crucial in providing the N required for seagrass photosynthesis and growth when its availability is limited^{29,30}. Diazotrophic bacteria have been detected in the rhizosphere of *P. oceanica*³¹ with high rates of root-associated N₂ fixation reported³². Analogous to many land plants that associate with diazotrophs, a recent study shows that *P. oceanica* lives in symbiosis with an N₂-fixing γ -proteobacterium in its roots, providing N in exchange for sugars, that can fully sustain plant biomass production during its primary growth season²⁹. Apart from this root-symbiosis, N₂ fixation has been shown to occur associated with all parts of *P. oceanica*, both above and below ground³³.

Overall, although rhizosphere N cycling has been the focus of extensive research, precise quantification of N transformations on seagrass leaves, as well as an evaluation of the effects of OA, are still lacking. Phyllospheric N₂ fixation can considerably contribute to the N demand of *P. oceanica* and to the N budget in the Mediterranean Sea^{29,30}. Besides N₂ fixation, we hypothesize that seagrass leaves could also be suitable sites for nitrification. For example, Ling et al.³⁴ found a diverse community of ammonia-oxidizing archaea (AOA) and bacteria (AOB) associated with different parts of the seagrass *Thalassia hemprichii*, including leaf tissues. Moreover, anoxic parts within μm to mm-thick biofilms on the leaf surface could provide potential microhabitats for N loss pathways, such as denitrification^{35,36} or anammox performed by groups such as Planctomycetes, which were found to dominate the microbiome of *P. oceanica* leaves at some locations³⁷.

Here, we investigate the effects of long-term natural OA occurring at volcanic CO₂ vents on the epiphytic prokaryotic community of *P. oceanica* leaves and quantify rates of the key N cycling processes by the plant phyllosphere. We test the effects of pH and the presence/absence of epiphytes in multifactorial laboratory incubations (see Supplementary Fig. 1), using N stable isotope tracers to quantify N₂ fixation, nitrification potential, and anammox and denitrification potential, and net nutrient fluxes to quantify assimilatory processes by leaves and epiphytes. We complement these analyses with 16 s rRNA gene amplicon sequencing to explore the diversity of the phyllosphere microbial community and the potential players involved in N transformation processes on seagrass leaves.

Results and discussion

Complete microbial N cycling occurs in the *P. oceanica* phyllosphere

Incubation experiments with ¹⁵N stable isotope labeling reveal that all key microbial N cycling processes occurred in the phyllosphere of *P. oceanica*, with microbial epiphytes contributing to a net N gain in all conditions by the holobiont. To quantify rates of N₂ fixation by the phyllosphere diazotrophic community, we incubated leaf sections with and without epiphytes in ¹⁵N₂-enriched seawater. We detected clear ¹⁵N₂ incorporation in epiphyte tissue in the light incubations, ranging from $0.12 \pm 0.05 \text{ nmol cm}^{-2} \text{ h}^{-1}$ (mean \pm SE) at the ambient site to $0.62 \pm 0.15 \text{ nmol N cm}^{-2} \text{ h}^{-1}$ at the vent site

(Fig. 1a). ¹⁵N₂ incorporation was 409% higher at the vent site ($F_{1,13} = 5.80$, $p = 0.03$, $R^2 = 0.52$) and in the same order of magnitude as N₂ fixation rates measured in situ in minimally disturbed *P. oceanica* meadows³⁸. Corresponding to dry weight-based rates of up to $131.08 \text{ nmol N g DW}^{-1} \text{ h}^{-1}$, these rates are also comparable to N₂ fixation rates measured by root symbionts of *P. oceanica* under ambient pH^{29,32}. Conversely, we observed significant ¹⁵N₂ incorporation in only one of four replicates in the dark. We did not observe a significant transfer of fixed N to the *P. oceanica* plant tissues in the limited time frame of the experiment, neither in the light nor in the dark (Supplementary Figs. 2 and 3).

We explored the potential of the phyllosphere microbiome to nitrify in ¹⁵N-NH₄⁺ incubation experiments. While there was a strong variability among samples (Supplementary Fig. 4), we found significant ($>2.5 \times \text{SD}$) potential nitrification rates (PNR) at the vent site when epiphytes were present (Fig. 1b), ranging from $0.031 \pm 0.007 \text{ pmol N cm}^{-2} \text{ h}^{-1}$ (mean \pm SE) in the dark to $0.058 \pm 0.004 \text{ pmol N cm}^{-2} \text{ h}^{-1}$ in the light. However, these rates were only marginal compared to the other N transformation processes. PNR was 86% higher in the light ($F_{1,13} = 67.00$, $p < 0.001$, $R^2 = 0.83$). In contrast, we found no significant PNR in incubations with epiphytes from the ambient site, neither in the light nor in the dark. The plant can compete with nitrifiers for N, as NH₄⁺ is typically readily taken up by *P. oceanica*³⁹, making the leaf phyllosphere a challenging environment for nitrifying prokaryotes. Our measurements of PNR in *P. oceanica* leaves are of relevance, as it indicates that a community of nitrifiers exists that can compete with the plant for NH₄⁺ uptake. However, with PNR of up to $0.058 \pm 0.004 \text{ pmol N cm}^{-2} \text{ h}^{-1}$, their net contribution to NH₄⁺ or NO₂⁻ oxidation contributes only marginally to the N budget of the *P. oceanica* phyllosphere.

Previous studies suggested that anoxic parts within thick biofilms on the surface of seagrasses could be suitable microhabitats for microbial-mediated N-loss pathways, such as denitrification and anammox^{35,36}. Using incubation experiments of leaf sections amended with ¹⁵N-NO₃⁻, we report ²⁹N₂ production rates ranging from $2.43 \pm 0.53 \text{ pmol N cm}^{-2} \text{ h}^{-1}$ at the ambient site in the dark to $7.14 \pm 2.07 \text{ pmol N cm}^{-2} \text{ h}^{-1}$ at the vent site in the light (Fig. 1c) when epiphytes were present. ²⁹N₂ production was 134% higher at the vent site ($F_{1,13} = 10.82$, $p = 0.006$, $R^2 = 0.39$), while the light/dark treatment had no effect. A significant production rate of ³⁰N₂ was only detected at the vent site in the light with epiphytes present ($18.84 \pm 3.33 \text{ pmol N cm}^{-2} \text{ h}^{-1}$; Fig. 1d). Based on these results, we calculated daily budgets of total N-N₂ loss (sum of ²⁹N₂ and ³⁰N₂ production) of up to $4.01 \pm 0.74 \text{ } \mu\text{mol N m}^{-2} \text{ d}^{-1}$ (or $0.401 \pm 0.074 \text{ nmol N cm}^{-2} \text{ d}^{-1}$) at the vent site. These rates are significant, and comparable to N loss rates reported from seagrass sediments by Salk et al.⁴⁰, who measured denitrification rates of $0.10 \text{ nmol N cm}^{-2} \text{ d}^{-1}$ and anammox rates of $0.43 \text{ nmol N cm}^{-2} \text{ d}^{-1}$. The presence of Planctomycetes and detectable rates of ²⁹N₂ in ¹⁵N-NO₃⁻ amended incubations suggest that anammox may play an important role as an N loss pathway on seagrass leaves.

P. oceanica can assimilate fixed N as NH₄⁺ or NO₃⁻³⁹ but shows a higher affinity for NH₄⁺⁴¹. While NH₄⁺ uptake rates were unaffected by the presence or absence of epiphytes (Supplementary Fig. 5a, b), NO₃⁻ consumption rates (Supplementary Fig. 5c, d) were increased by 147–270% in the presence of epiphytes. This is probably due to active NO₃⁻ uptake because NO₃⁻ loss via denitrification or anammox and nitrification activity was three orders of magnitude lower (Fig. 1c, d). This suggests that epiphytes may preferentially use this form of N as a strategy to avoid competition for N with the plant, combining active NO₃⁻ uptake and N₂ fixation.

Distinct microbial communities contribute to seagrass phyllosphere N cycling

The 16 s rRNA gene amplicon sequencing of the phyllosphere-associated microbiome revealed a diverse microbial community differing from the water column but not between ambient and vent pH (see Supplementary Fig. 6 and Supplementary Table 1), and including many members potentially involved in N transformation processes on *P. oceanica* leaves.

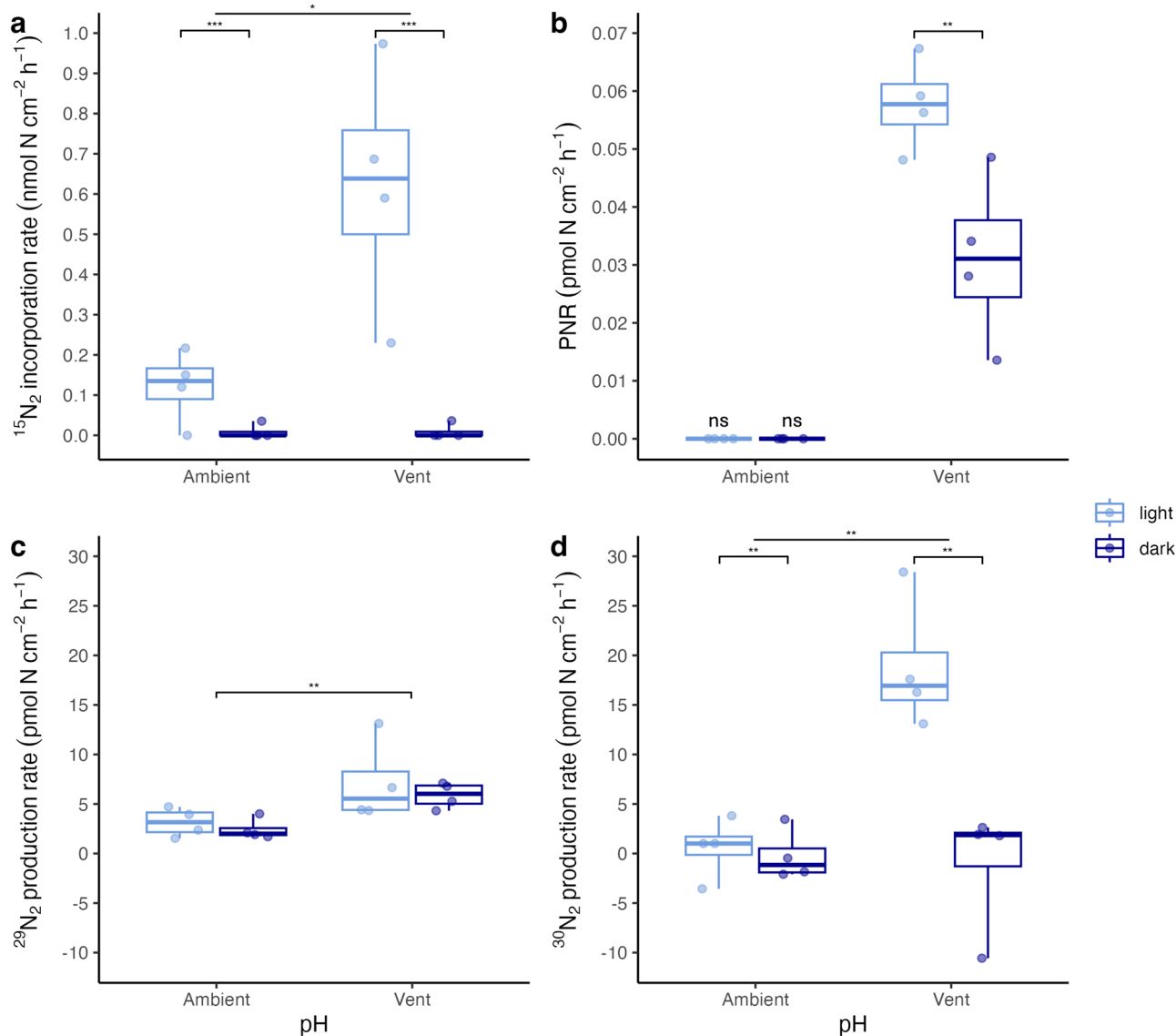


Fig. 1 | Epiphyte-mediated nitrogen transformations in light and dark incubations from the ambient and vent site. Epiphytic ¹⁵N₂ fixation rates (a), potential nitrification rates (PNR) in incubations with epiphytes (b), ²⁹N₂ and ³⁰N₂ production rate in incubations with epiphytes (c, d). The center line denotes the median value

(50th percentile), the box contains the 25th to 75th percentiles. Whiskers mark the 5th and 95th percentiles. Letters indicate significant differences between treatments, ns indicates enrichment was not significant, $n = 4$.

The leaves were dominated by the phylum *Proteobacteria* with the classes *Alphaproteobacteria* (20–22%) and *Gammaproteobacteria* (9–15%) across both pH sites (Fig. 2). Among the predominant orders were *Rhodobacterales* (9%), which are commonly found as first colonizers on marine surfaces and seagrasses, probably due to their ability to be opportunistic and persist in rapidly changing environments^{42–44}. About 1.5% of this clade were identified as *Epibacterium*, a genus of common bacteria in coastal areas that have the potential to assimilate ammonium and that also expresses antibacterial activity towards other marine bacteria⁴⁵. Other ammonia oxidizers, such as the strain HIMB11 were identified in the water column⁴⁶. *Rhodobacterales* also include (putative) N₂ fixers in both terrestrial⁴⁷ and marine^{48,49} environments. We found *Rhizobiales* accounting for 5% of the total leaf community, a taxonomic order that includes a diversity of N₂-fixing microbes that form symbiotic relationships with terrestrial plants⁵⁰ and known for promoting plant health and growth⁵¹. One of the identified genera within this clade was *Pseudovibrio*, a common member of animal and macrophyte holobionts, with the capacity to undergo complete denitrification and, in some species, assimilatory nitrate

reduction and probably another regulator of the microbial community through their antibiotic metabolite production⁵².

Cyanobacteria accounted for 2–14% of the total leaf community (Fig. 2). Especially the orders *Phormidiales* and *Cyanobacteriales* had a large effect in the differential abundance analysis (Fig. 3). Higher N₂ fixation rates under light conditions suggest a diazotrophic community dominated by species that can cope with O₂ production from daytime photosynthesis, which would otherwise irreversibly inhibit the enzyme nitrogenase. Among the genera that can sustain N₂ fixation in the light^{53,54}, the leaves from both pH regimes comprised sequences for *Schizothrix* (0.22% on leaves vs. 0.01% in the water column) and *Trichodesmium* (up to 0.5% on leaves vs. 0.002% in the water column).

Among the predominant orders in the phylum *Bacteroidota* (17%) was the order *Flavobacteriales* (8%), members of which are also frequently found as early colonizers on marine surfaces and seagrasses^{43,44}. In particular, some photosynthetic and light-dependent members of *Bacteroidota* that harbor the *nifH* gene, e.g., *Chlorobaculum* and *Chlorobium*, are found more abundantly on leaves than in the water column³⁸. Other heterotrophic bacterial N₂ fixers that may depend on seagrass photosynthetic exudates³⁸

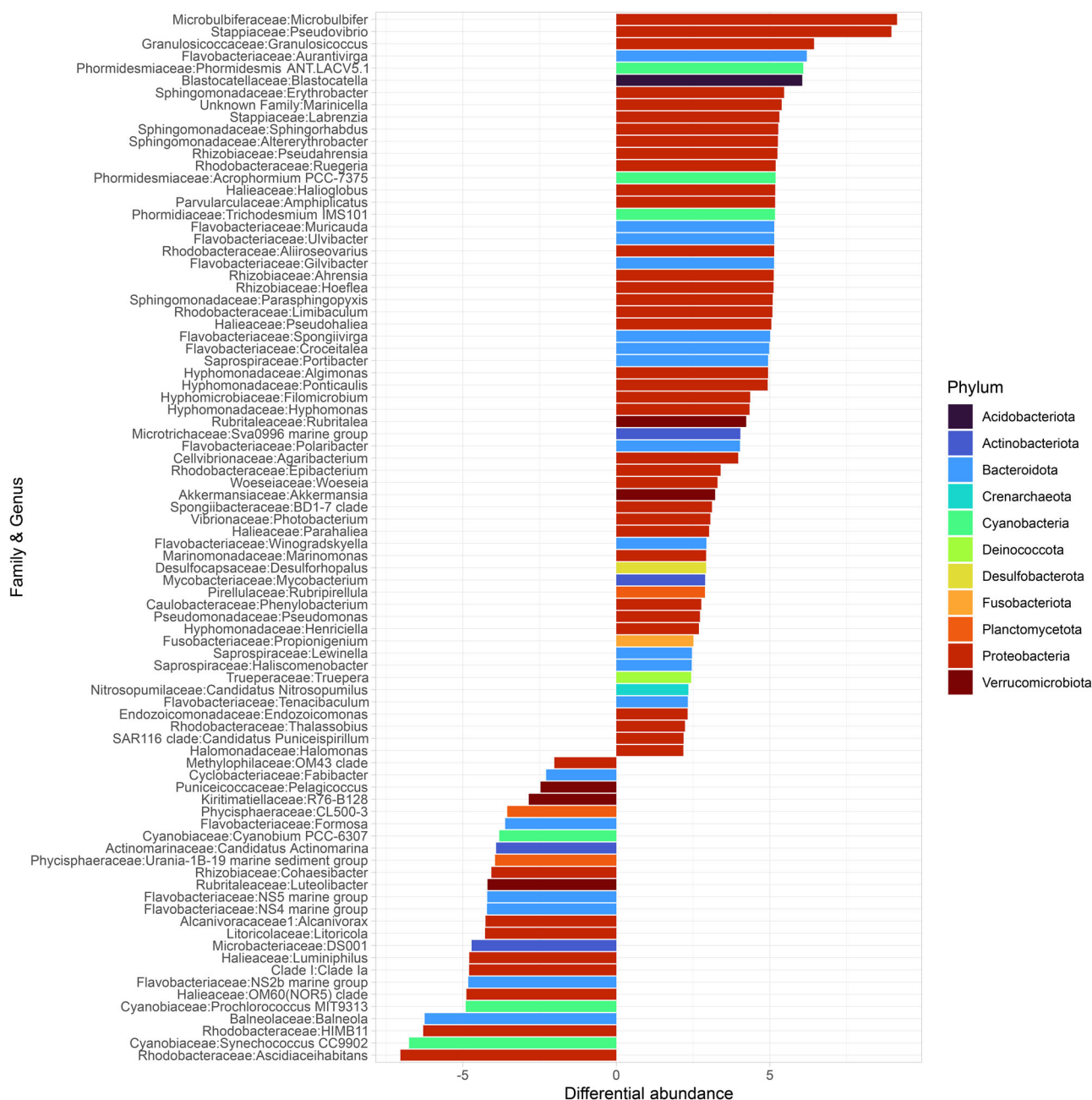


Fig. 3 | Differential taxonomic order abundance in pooled leaf and water column samples. Positive values mean differential abundance in the leaves and negative values in the water column.

daily primary production of the *P. oceanica* holobiont (plant + epiphytes) that can be supported by leaf-associated N₂ fixation (Fig. 4A, B).

Although NCP, and thus the seagrass N demand, was higher under OA, the contribution of N₂ fixation to meeting this demand was increased at the vent pH. N₂ fixation contributed with 169 ± 71 mmol N m⁻² d⁻¹ to 35% of the seagrass N demand at ambient pH and with 493 ± 129 mmol N m⁻² d⁻¹ to 45% at vent pH (Fig. 4). The contribution of N₂ fixation to the seagrass N demand has been reported to be highly variable over seasonal e.g., refs. ^{38,79}, and spatial³⁸ gradients. Integrating the seasonal values over a year, Agawin et al.³⁸ calculated that ca. 15% of the annual plant N demand can be provided by aboveground N₂ fixation in *P. oceanica* meadows. Further research (e.g., using NanoSIMS or longer-term incubations) should investigate how much of the N fixed by the epiphytic diazotrophs is actually transferred to the plant host.

A large fraction of the *P. oceanica* holobiont N demand was obtained through NH₄⁺ uptake with 829 ± 87 mmol N m⁻² d⁻¹ at the ambient and 3376 ± 461 mmol N m⁻² d⁻¹ at the vent site (Fig. 4). NH₄⁺ uptake was considered being plant-mediated, because the presence of epiphytes had no significant effect (Supplementary Fig. 5). NO₃⁻ uptake, primarily attributed to the epiphytic community, contributed with 159 ± 37 mmol N m⁻² d⁻¹ at the ambient and 555 ± 139 mmol N m⁻² d⁻¹ at the vent site. NO₃⁻ uptake rates were comparable to the annual average NO₃⁻ leaf uptake by Lepoint et al.³⁹ (1.2 g N m⁻² yr⁻¹ = 235 mmol N m⁻² d⁻¹). Conversely, NH₄⁺ uptake rates were higher than their maximum values obtained in spring months (1300 mg N m⁻² h⁻¹ = 2227 mmol N m⁻² d⁻¹)³⁸. However, Lepoint et al. also show that large seasonal differences can occur, with values ranging from 0 to 2227 mmol N m⁻² d⁻¹³⁹. The total N gain (N₂ fixation + NH₄⁺ and NO₃⁻ uptake - N loss) was 1115 ± 194 mmol N m⁻² d⁻¹ at the ambient and 4410 ± 727 mmol N m⁻² d⁻¹ at the vent site. Thus, OA tipped the balance

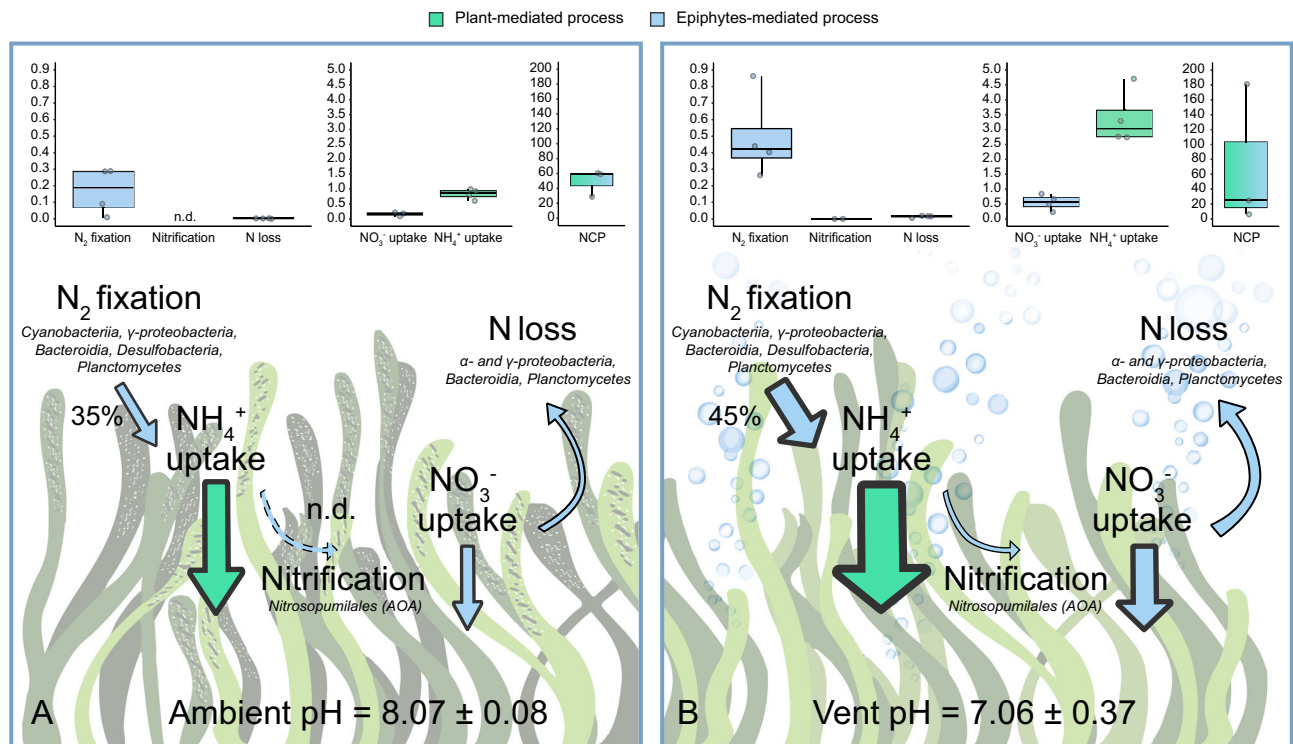


Fig. 4 | Overview of N cycling processes under ambient and vent pH conditions. The metabolic rates (in $\text{mmol m}^{-2} \text{ meadow area d}^{-1}$) for plant- and epiphyte-mediated processes under ambient (A) and vent (B) pH conditions, based on a 12:12 h light and dark cycle, are depicted in the upper portion of each panel. Data distribution is shown in a box plot format, with the center line denoting the median value (50th percentile), the box encapsulating the interquartile range (25th to 75th percentiles),

and whiskers indicating the 5th and 95th percentiles. Nitrification was not detectable (n.d.) at the ambient site. The lower portion of each panel employs arrow size to convey the relative differences in N cycling processes. Additionally, the % contribution of N₂ fixation to the estimated N demand of the plant, as well as relevant taxa in the microbial community for each N cycling process, are provided for further context.

decisively in favor of increased N gain. It is crucial for other studies to investigate similar processes in other natural CO₂ vent sites and for other seagrass species to broaden our understanding of these phenomena.

Taken together, our results show that major N cycling processes occur on *P. oceanica* leaves, and that epiphytes contribute to net N uptake by the holobiont. Ocean acidification occurring at the investigated volcanic CO₂ vent accelerates N cycling, while the prokaryotic community structure remains largely unaffected. At a vent pH (~7), high rates of microbial daylight N₂ fixation on the phyllosphere of *P. oceanica* can partially sustain the increased C-fixation and thus N demand of the holobiont. Further experiments at comparable sites with reduced pH should investigate whether our results can be generalized to a broader spatial scale. Access to diverse N sources may help to avoid competition within the holobiont. Adaptation of marine plants to environmental changes is fundamental for their survival; here we show that functional plasticity of their N-cycling microbiome is a key factor in regulating seagrass holobiont functioning on a changing planet.

Methods

Study area and sampling

The study area is located at the islet of Castello Aragonese on the northeastern coast of the island of Ischia (Tyrrhenian Sea, Italy). This site is characterized by the presence of submarine CO₂ vents of volcanic origin, which naturally generate a gradient in CO₂ concentration and pH, without affecting the surrounding water temperature or salinity^{80,81}. Around the islet, meadows of *P. oceanica* occur at depths of 0.5–3 m, also extending into vent zones with low pH. We selected two sites characterized by different pH regimes (vent pH = 7.80 ± 0.14; ambient pH = 8.08 ± 0.04; Supplementary Table 3) at approximately 3 m water depth. We restricted our study locations to these sites, because not many vent sites have comparable levels of CO₂, depth,

light, and hydrodynamics. Increasing the number of locations would have increased confounding factors, potentially affecting the reliability and consistency of our data. The vent pH site was located in a vent area on the south side (40°43'50.5"N 13°57'47.2"E) and the ambient pH site was located on the north side of the bridge (40°43'54.8"N 13°57'47.1"E).

For the incubation experiments, shoots of *P. oceanica* were collected at each site on three days in September 2019 and transported directly to the laboratory. Sections of the central part of the leaf (3 cm in length) were cut off, selecting leaves with homogeneous epiphyte coverage, and avoiding heavily grazed and senescent parts of the plant, as described in Berlinghof et al.¹². Macro-epiphytes and biofilm were carefully removed from half of the seagrass leaves with a scalpel, ensuring the removal of the majority of microbial epiphytes and taking special care not to damage the plant tissue. Leaf sections from the vent pH and ambient pH sites, with epiphytes present ($n = 4$) or removed ($n = 3$), were used for dark and incubations. Focusing on the leaves allowed us to control for the community composition within the phyllosphere exposed to oxygen-rich seawaters and avoiding contrasting processes occurring between the mainly oxidized aboveground phyllosphere and the mainly reduced belowground rhizosphere.

Samples for microbial community analysis were collected in October 2019 at the vent ($n = 3$) and ambient site ($n = 4$) described above. Before disturbing the plants, we collected 5 L of seawater from the water column above the plants at each site. Whole seagrass plants were collected, and the central part of the leaf was cut off with sterile tools, washed with sterile NaCl solution [0.8% m/v] to remove loosely attached microorganisms, and transferred to 15 mL falcon tubes with sterile tweezers. The falcon tubes were kept in dry ice during transport to the laboratory (SZN Villa Dohrn, Ischia, Italy) and then stored at -20 °C. In the laboratory, the seawater was immediately filtered on 0.2 μm cellulose nitrate membrane filters ($n = 2$ at each site) and the filters were stored at -20 °C until further genetic analysis.

Prokaryotic DNA extraction, amplification, and sequencing

DNA from seagrass and seawater samples was extracted using the Qiagen DNeasy PowerSoil Kit (Qiagen). For seawater, the entire membrane filters were used, while for seagrass, we cut approximately 1 g of the central part of the leaf. Leaf samples were placed into 2 mL vials containing 600 μL of sterile NaCl solution [0.8% m/v] and were vortexed three times for 30 s according to the protocol of the Seagrass Microbiome Project (<https://seagrassmicrobiome.org>). The solution was transferred to the Powerbead columns (Qiagen) and then processed according to the manufacturer's instructions with slight modifications to increase DNA yield and quality, as described in Basili et al.⁸² The extracted DNA samples were quantified using a microvolume spectrophotometer (Thermo Scientific NanoDrop 2000c) and stored at -20°C until processing.

Illumina MiSeq sequencing (2 \times 300 bp paired-end protocol) of the hypervariable V4 region of the 16S rRNA gene was performed using the 515FB and 806RB bacteria- and archaea-specific primers⁸³. The primers were removed from the raw sequence data using cutadapt v2.8⁸⁴ and the fastq files were processed using the R package DADA2^{85,86}. Quality filtering and denoising of the trimmed fastq files was performed using the following parameters: "truncLen = c(200, 200), maxEE = c(2, 2), truncQ = 2, ndmaxN = 0). Paired-end reads were then merged into amplicon sequence variants (ASVs); chimeric sequences were identified and removed. Prokaryotic taxonomy assignment was performed using the SILVA v138⁸⁷ database. The complete pipeline is openly available in the research compendium accompanying this paper at <https://github.com/luismmontilla/embrace>. The sequences are available in the NCBI SRA database as the BioProject ID PRJNA824287.

Bioinformatics and data analysis of the sequencing data

The ASV matrix was analyzed as a compositional dataset, as described in detail in other works^{88,89}. Briefly, we transformed the raw pseudo-counts using the centered-log ratio to handle the data in a Euclidean space. We then tested the null hypothesis of no effect of the factors described above on the prokaryotic community associated with *P. oceanica* using a permutation-based multivariate analysis of variance (PERMANOVA) derived from a Euclidean distance matrix. We performed this test using the *vegan* package for R^{90,91}. In addition, we performed a differential abundance analysis of the ASVs (pooled leaf vs water column samples) using the ANOVA-like differential expression method implemented in the ALDEX2 package for R⁹². This algorithm produces consistent results, whereas other analyses can be variable depending on the parameters set by the researcher or required by the dataset⁹³.

Dinitrogen fixation

The $^{15}\text{N}_2$ -enriched seawater addition method was used to determine N_2 fixation rates⁹⁴. The $^{15}\text{N}_2$ gas (Cambridge Isotope Laboratories Inc.) was tested negative for contamination with ^{15}N -labeled ammonium. Stock solutions of 0.22 μm filtered and $^{15}\text{N}_2$ -enriched water from the two study sites (vent and ambient pH) were prepared and gently transferred to 24 mL glass vials to minimize gas exchange with the atmosphere. Subsequently, one section of a seagrass leaf with ($n = 4$) and without epiphytes ($n = 3$) was added per vial and the vials were sealed without leaving any headspace. Additionally, vials with 0.22 μm filtered but unenriched site water containing leaves with epiphytes served as controls to account for potential variation in natural abundance of ^{15}N in epiphytes or leaves ($n = 3$, see also Supplementary Fig. 1 for the experimental design). The vials were incubated on a shaker (Stuart Orbital Shaker SSL1; 30 rpm); vials for dark incubations were covered with aluminum foil. Incubations were performed in a temperature-controlled room at 22°C . After an incubation period of $T_0 = 0$ h, $T_1 = 5$ h, and $T_2 = 9$ h light/ 8 h dark, three or four vials from each treatment were opened for sampling. At the beginning and end of the incubation, oxygen concentrations in the incubation vials were measured without opening the vials using a fiber-optic oxygen sensor with sensor spots (FireStingO2, PyroScience), and pH was measured using a pH meter (Multi 3430, WTW).

For tissue analysis, epiphytes were removed from seagrass leaves with a scalpel and transferred separately into Eppendorf tubes and freeze-dried for 72 h. They were then homogenized in a mortar, weighed, and transferred into tin cups to determine carbon (%C) and nitrogen content (%N), and ^{15}N incorporation. Water samples were transferred to 12 mL exetainers (Labco Ltd) and fixed with 200 μL of 7 M ZnCl_2 for $^{29}\text{N}_2$ and $^{30}\text{N}_2$ analyses to calculate atom% excess of the medium. In addition, samples for the analysis of dissolved inorganic nitrogen (DIN: NH_4^+ , NO_2^- , NO_x^-) and PO_4^{3-} were transferred to 20 mL HDPE vials and stored at -20°C until further analysis.

Carbon (%C) and nitrogen (%N) content and the isotopic composition ($\delta^{13}\text{C}$, $\delta^{15}\text{N}$) in seagrass leaves and epiphyte tissue were analyzed by isotope ratio mass spectrometry (IRMS, Delta plus V, Thermo Scientific) coupled to an elemental analyzer (Flash EA1112, Thermo Scientific) at Aarhus University (Denmark). $^{15}\text{N}_2$ fixation rates were calculated according to Montoya et al.⁹⁵:

$$^{15}\text{N}_{\text{excess}} = ^{15}\text{N}_{\text{sample}} - ^{15}\text{N}_{\text{NA}} \quad (\text{I})$$

$$\text{N}_2 \text{ fixation} = (\text{atom}\%(^{15}\text{N}_{\text{excess}}) / \text{atom}\%(^{15}\text{N}_{\text{medium}})) \times (\text{PN}_{\text{sample}} / t) \quad (\text{II})$$

$^{15}\text{N}_{\text{sample}}$ is the ^{15}N content of the samples after exposure to $^{15}\text{N}_2$ enriched seawater, and $^{15}\text{N}_{\text{NA}}$ is the ^{15}N content in natural abundance samples without $^{15}\text{N}_2$ exposure. The enrichment of samples ($^{15}\text{N}_{\text{excess}}$) was considered significant for samples with a value greater than 2.5 times the standard deviation of the mean of the natural abundance samples. $^{15}\text{N}_{\text{medium}}$ is the enrichment of the incubation medium at the end of the incubations. With our approach, we achieved an enrichment of ~ 16.0 atom % ^{15}N in the incubation vials. $\text{PN}_{\text{sample}}$ is the N content of the sample (μg), and t represents the incubation time (h). $^{15}\text{N}_2$ fixation rates were normalized per seagrass leaf area (cm^2). The C:N molar ratio was determined as: $\text{C:N} = (\% \text{C}/12) / (\% \text{N}/14)$.

Dissolved nutrient concentrations (NH_4^+ , NO_2^- , NO_x^- , PO_4^{3-}) were measured with a continuous flow analyzer (Flowsys, SYSTEA S.p.A.). NO_3^- concentrations were calculated as the difference between NO_x^- and NO_2^- . Subsequently, nutrient fluxes were calculated as the difference between final and initial nutrient concentrations, corrected for controls, and normalized to leaf area.

Potential Nitrification rates

Nitrification potential was determined using stock solutions of 0.22 μm filtered water from the study sites (vent and ambient pH site) with an ambient NH_4^+ concentration of 0.65 μM that was enriched with $^{15}\text{NH}_4^+$ (≥ 98 atom % ^{15}N) to a final concentration of 20 μM . The incubation was performed as described above (see also Supplementary Fig. 1 for the experimental design) with sampling times at $T_0 = 0$ h, $T_1 = 2$ h, $T_2 = 5$ h, and $T_3 = 9$ h light/ 8 h dark. Water samples were filtered at 0.22 μm , transferred to 15 mL polypropylene tubes, and stored at -20°C for the analysis of NO_3^- production. Vials with 0.22 μm filtered site water with 20 μM $^{15}\text{NH}_4^+$ but without leaves served as controls for background microbial activity in the water column ($n = 3$).

Isotopic samples for $^{15}\text{NO}_3^-$ production were analyzed by isotope ratio mass spectrometry (IRMS) using a modified version of the Ti(III) reduction method described by Altabet et al.⁹⁶ Sample aliquots for nitrification analysis (3 mL) were acidified by adding 10 μL of 2.5 nM sulfanilic acid in 10% HCl to each 1 mL of sample, then added to 3 mL of the international standard USGS-32 ($\delta^{15}\text{N} = +180\text{‰}$) in a 12 mL exetainer, so that the final concentration of USGS-32 was 0.1 ppm $\text{NO}_3\text{-N}$ ($\sim 7 \mu\text{M}$ NO_3^-). After combining the sample with the standard, the exetainer headspace was flushed with argon for 2 min. NO_3^- was then converted to nitrous oxide (N_2O) for stable N isotope analysis by adding 200 μL zinc-treated 30% TiCl_3 . The exetainers were immediately sealed with a gas-tight, pierceable, chlorobutyl rubber septum and the final reaction volume was 6.15 mL. The Ti(III)-treated samples were left at room temperature for >12 h to convert NO_3^- to

N₂O. The headspace of the exetainer was sampled with a double-holed needle using a CTC PAL autosampler and a modified flush-fill line of a GasBench device (Thermo Scientific). The flush rate was ca. 25 mL min⁻¹ and the flushing time was 5.5 min. The headspace sample was passed through a magnesium perchlorate and ascarite trap to remove water and CO₂, respectively, and then collected in a sample loop (50 cm PoraPlot Q; ϕ = 0.53 mm; Restek) submersed in liquid nitrogen. N₂O in the sample was then separated from CO₂ and other gases by injecting onto a Carboxen 1010 PLOT column (30 m × 0.53 mm, 30 μ m film thickness, Supelco; temp = 90 °C, flow rate 2.6 mL min⁻¹) with helium as carrier gas. The sample was then transferred to a MAT253 PLUS IRMS via a Conflo interface (ThermoScientific). $\delta^{15}\text{N}$ values were determined relative to the N₂O working gas, and then corrected for linearity according to the peak height relationship and the titanium-to-sample ratio⁹⁶; the absolute value of the linear correction term was <1.3‰ for all samples. The corrected values were then normalized to the $\delta^{15}\text{N}$ -air scale by simultaneous analysis of the international standards USGS32, USGS34, and USGS35. The $\delta^{15}\text{N}$ value of NO₃⁻ in the sample was finally determined via a mass balance of the relative NO₃⁻ concentrations of the sample and USGS32, the measured $\delta^{15}\text{N}$ value of the mixture, and the accepted $\delta^{15}\text{N}$ value of USGS32. The external precision of the $\delta^{15}\text{N}$ measurement (\pm one standard deviation of the mean) determined for an in-house standard was 1.1‰.

Potential nitrification rates (PNR) were calculated using an equation modified from Beman et al.²⁵:

$$^{15}\text{N}_{\text{excess}} = ^{15}\text{N}_t - ^{15}\text{N}_0 \quad (\text{III})$$

$$\text{PNR} = (\text{atom}\%(^{15}\text{N}_{\text{excess}})/\text{atom}\%(^{15}\text{N}_{\text{medium}})) \times ([\text{NO}_3^-]/t) \quad (\text{IV})$$

$^{15}\text{N}_t$ is the ^{15}N content of the samples in the NO₃⁻ pool measured at time t , and $^{15}\text{N}_0$ is the ^{15}N content in the NO₃⁻ pool measured at the beginning of the incubations. The enrichment of samples ($^{15}\text{N}_{\text{excess}}$) was considered significant for samples with a value greater than 2.5 times the standard deviation of the mean of the T₀ samples. $^{15}\text{N}_{\text{medium}}$ is the enrichment of the incubation medium at the end of the incubations. Based on the NH₄⁺ concentrations measured before and after the addition of $^{15}\text{NH}_4^+$, this resulted in a theoretical enrichment of ~95.9 atom % ^{15}N in the incubation medium. [NO₃⁻] is the concentration of NO₃⁻ (μM) and t is the incubation time (h). Potential nitrification rates were normalized per seagrass leaf area (cm²) and corrected for the rates in control incubations without organisms.

Potential anammox and denitrification rates

To determine the rates of N loss via N₂ production (combined denitrification and anammox), stock solutions of 0.22 μm filtered water from the two study sites (vent and ambient pH) with an ambient NO₃⁻ concentration of 1.94 μM were enriched with $^{15}\text{NO}_3^-$ (≥ 98 atom % ^{15}N) to a final concentration of 10 μM . The incubation was performed as described above (see also Supplementary Fig. 1 for the experimental design), with sampling times at T₀ = 0 h, T₁ = 2 h, T₂ = 5 h, and T₃ = 9 h light/ 8 h dark. Vials with 0.22 μm filtered site water from each of the study sites with 10 μM $^{15}\text{NO}_3^-$ but without leaves served as controls for background microbial activity in the water column ($n = 3$). Water samples were transferred into 12 mL exetainers and fixed with 200 μL of 7 M ZnCl₂ for $^{29}\text{N}_2$ and $^{30}\text{N}_2$ analyses.

Isotopic samples for $^{29}\text{N}_2$ and $^{30}\text{N}_2$ production were analyzed by gas chromatography-isotope ratio mass spectrometry (GasBench, Thermo Scientific). $^{29}\text{N}_2$ and $^{30}\text{N}_2$ concentrations were calculated via linear regression of a standard curve with N₂ air standards. Production rates of ^{15}N -enriched N₂ gas were calculated from the difference in $^{29}\text{N}_2$ or $^{30}\text{N}_2$ concentrations between T₁ (2 h) and T₂ (5 h), as we observed a lag phase from T₀ to T₁. Because the changes in $^{29}\text{N}_2$ and $^{30}\text{N}_2$ concentrations were very small (Supplementary Table 4), we decided to report $^{29}\text{N}_2$ and $^{30}\text{N}_2$ production rates instead of further transforming the data to calculate denitrification or anammox rates. $^{29}\text{N}_2$ and $^{30}\text{N}_2$ production rates were normalized to seagrass leaf area (cm²) and corrected for the rates in control incubations without organisms.

Holobiont N demand calculations

To calculate daily metabolic rates of plant and epiphyte-mediated N cycling processes, we integrated rates of N₂ fixation, nitrification potential, N loss (denitrification and anammox), NO₃⁻, and NH₄⁺ uptake in the light and dark incubations assuming a daily 12:12 h light/dark cycle. We used net community productivity (NCP) from Berlinghof et al.¹² (using a photosynthetic quotient of 1), C:N ratios (Supplementary Fig. 8), average leaf density and dry weight per leaf at the ambient and vent site (Supplementary Table 5) to calculate daily rates (in mmol N m⁻² meadow area d⁻¹) at vent and ambient pH. We further calculated the potential percentage of daily primary production of the seagrass holobiont (plant + epiphytes) that can be supported by leaf-associated N₂ fixation.

Statistics and reproducibility

For the incubation experiments, we used central sections of *P. oceanica* leaves from the vent and ambient pH site with epiphytes present ($n = 4$) or removed ($n = 3$) in dark and incubations (see Supplementary Fig. 1). Samples were not measured repeatedly; for every sampling timepoint a new incubation vial was opened and measured.

We tested for normality and homogeneity of variances before each analysis using Shapiro–Wilk’s and Levene’s tests and transformed data or removed outliers if normality and homogeneity of variances were not met. We tested the effects of pH (vent pH vs. ambient pH), treatment (with and without epiphytes), and their interaction on the $^{15}\text{N}_2$ incorporation rates, potential nitrification rates (PNR), $^{29}\text{N}_2$ and $^{30}\text{N}_2$ production rates, and the nutrient fluxes using two-way ANOVAs (type II). We tested the effects of pH (vent pH vs. ambient pH) on the C:N ratios of leaves and epiphytes using a one-way ANOVA (type II). All statistical analyses were performed with R⁸⁵ (version 4.1.2) using the packages *car* and *emmeans*.

Reporting summary

Further information on research design is available in the Nature Portfolio Reporting Summary linked to this article.

Data availability

The source data for all figures and tables can be found in Supplementary Data. Raw sequencing data supporting the results of this study have been deposited in the NCBI SRA database with the BioProject accession code: PRJNA824287.

Received: 2 June 2023; Accepted: 5 March 2024;

Published online: 19 March 2024

References

- Hemminga, M. A. & Duarte, C. M. *Seagrass Ecology*. *Seagrass Ecology* (Cambridge University Press, 2000). <https://doi.org/10.1017/cbo9780511525551>.
- Björk, M., Short, F. T., Mcleod, E. & Beer, S. *Managing seagrasses for resilience to climate change*. (IUCN, Gland, Switzerland, 2008).
- Hyman, A. C., Frazer, T. K., Jacoby, C. A., Frost, J. R. & Kowalewski, M. Long-term persistence of structured habitats: seagrass meadows as enduring hotspots of biodiversity and faunal stability. *Proc. R. Soc. B* **286**, 20191861 (2019).
- Fourqurean, J. W. et al. Seagrass ecosystems as a globally significant carbon stock. *Nat. Geosci.* **5**, 505–509 (2012).
- Duarte, C. M., Kennedy, H., Marbà, N. & Hendriks, I. Assessing the capacity of seagrass meadows for carbon burial: Current limitations and future strategies. *Ocean Coast Manag.* **83**, 32–38 (2013).
- Hendriks, I. E. et al. Photosynthetic activity buffers ocean acidification in seagrass meadows. *Biogeosciences* **11**, 333–346 (2014).
- Lacoue-Labarthe, T. et al. Impacts of ocean acidification in a warming Mediterranean Sea: An overview. *Reg. Stud. Mar. Sci.* **5**, 1–11 (2016).
- Goyet, C. et al. Thermodynamic forecasts of the Mediterranean Sea acidification. *Mediterr. Mar. Sci.* **17**, 508–518 (2016).

9. Koch, M., Bowes, G., Ross, C. & Zhang, X.-H. Climate change and ocean acidification effects on seagrasses and marine macroalgae. *Glob. Chang Biol.* **19**, 103–132 (2013).
10. Cox, T. E. et al. Effects of ocean acidification on *Posidonia oceanica* epiphytic community and shoot productivity. *J. Ecol.* **103**, 1594–1609 (2015).
11. Hernán, G. et al. Seagrass (*Posidonia oceanica*) seedlings in a high-CO₂ world: from physiology to herbivory. *Sci. Rep.* **6**, 38017 (2016).
12. Berlinghof, J. et al. The role of epiphytes in seagrass productivity under ocean acidification. *Sci. Rep.* **12**, 6249 (2022).
13. Cox, T. E. et al. Effects of in situ CO₂ enrichment on structural characteristics, photosynthesis, and growth of the Mediterranean seagrass *Posidonia oceanica*. *Biogeosciences* **13**, 2179–2194 (2016).
14. Scartazza, A. et al. Carbon and nitrogen allocation strategy in *Posidonia oceanica* is altered by seawater acidification. *Sci. Total Environ.* **607**, 954–964 (2017).
15. Donnarumma, L., Lombardi, C., Cocito, S. & Gambi, M. C. Settlement pattern of *Posidonia oceanica* epibionts along a gradient of ocean acidification: an approach with mimics. *Mediterr. Mar. Sci.* **15**, 498–509 (2014).
16. Mecca, S., Casoli, E., Ardizzone, G. & Gambi, M. C. Effects of ocean acidification on phenology and epiphytes of the seagrass *Posidonia oceanica* at two CO₂ vent systems of Ischia (Italy). *Mediterr. Mar. Sci.* **21**, 70–83 (2020).
17. Gravili, C., Cozzoli, F. & Gambi, M. C. Epiphytic hydroids on *Posidonia oceanica* seagrass meadows are winner organisms under future ocean acidification conditions: evidence from a CO₂ vent system (Ischia Island, Italy). *Eur. Zool. J.* **88**, 472–486 (2021).
18. Hemminga, M. A. & Harrison, P. G. & Van Lent, F. The balance of nutrient losses and gains in seagrass meadows. *Mar. Ecol. Prog. Ser.* **71**, 85–96 (1991).
19. Kuypers, M. M. M., Marchant, H. K. & Kartal, B. The microbial nitrogen-cycling network. *Microb. Biogeochem.* **16**, 263–276 (2018).
20. Wyatt, N. J. et al. Effects of high CO₂ on the fixed nitrogen inventory of the Western English Channel. *J. Plankton Res.* **32**, 631–641 (2010).
21. Wannicke, N., Frey, C., Law, C. S. & Voss, M. The response of the marine nitrogen cycle to ocean acidification. *Glob. Chang Biol.* **24**, 5031–5043 (2018).
22. Hutchins, D. A., Mulholland, M. R. & Fu, F. Nutrient Cycles and Marine Microbes in a CO₂-Enriched Ocean. *Oceanography* **22**, 128–145 (2009).
23. Levitan, O. et al. Elevated CO₂ enhances nitrogen fixation and growth in the marine cyanobacterium *Trichodesmium*. *Glob. Chang. Biol.* **13**, 531–538 (2007).
24. Kranz, S. A. et al. Combined Effects of CO₂ and Light on the N₂-Fixing Cyanobacterium *Trichodesmium* IMS101: Physiological Responses. *Plant Physiol.* **154**, 334–345 (2010).
25. Beman, J. M. et al. Global declines in oceanic nitrification rates as a consequence of ocean acidification. *PNAS* **108**, 208–213 (2011).
26. Ugarelli, K., Chakrabarti, S., Laas, P. & Stingl, U. The Seagrass Holobiont and Its Microbiome. *Microorganisms* **5**, 81 (2017).
27. Tarquinio, F., Hyndes, G. A., Laverock, B., Koenders, A. & Sävström, C. The seagrass holobiont: Understanding seagrass-bacteria interactions and their role in seagrass ecosystem functioning. *FEMS Microbiol. Lett.* **366**, 1–15 (2019).
28. Pfister, C. A. et al. Microbial associates of an endemic Mediterranean seagrass enhance the access of the host and the surrounding seawater to inorganic nitrogen under ocean acidification. *Sci. Rep.* **13**, 19996 (2023).
29. Mohr, W. et al. Terrestrial-type nitrogen-fixing symbiosis between seagrass and a marine bacterium. *Nature* **2021**, 1–5 (2021) <https://doi.org/10.1038/s41586-021-04063-4>.
30. Agawin, N. S. R. et al. Significant nitrogen fixation activity associated with the phyllosphere of Mediterranean seagrass *Posidonia oceanica*: first report. *Mar. Ecol. Prog. Ser.* **551**, 53–62 (2016).
31. Garcias-Bonet, N., Arrieta, J. M., Duarte, C. M. & Marbà, N. Nitrogen-fixing bacteria in Mediterranean seagrass (*Posidonia oceanica*) roots. *Aquat. Bot.* **131**, 57–60 (2016).
32. Lehnen, N. et al. High rates of microbial dinitrogen fixation and sulfate reduction associated with the Mediterranean seagrass *Posidonia oceanica*. *Syst. Appl. Microbiol.* **39**, 476–483 (2016).
33. Agawin, N. S. R., Ferriol, P. & Sintes, E. Simultaneous measurements of nitrogen fixation in different plant tissues of the seagrass *Posidonia oceanica*. *Mar. Ecol. Prog. Ser.* **611**, 111–127 (2019).
34. Ling, J. et al. Community Composition and Transcriptional Activity of Ammonia-Oxidizing Prokaryotes of Seagrass *Thalassia hemprichii* in Coral Reef Ecosystems. *Front. Microbiol.* **9**, 7 (2018).
35. Noisette, F., Depetris, A., Kühl, M. & Brodersen, K. E. Flow and epiphyte growth effects on the thermal, optical and chemical microenvironment in the leaf phyllosphere of seagrass (*Zostera marina*). *J. R. Soc. Interface* **17**, 20200485 (2020).
36. Brodersen, K. E. & Kühl, M. Effects of Epiphytes on the Seagrass Phyllosphere. *Front. Mar. Sci.* **9**, 1–10 (2022).
37. Kohn, T. et al. The Microbiome of *Posidonia oceanica* Seagrass Leaves Can Be Dominated by Planctomycetes. *Front. Microbiol.* **11**, 1458 (2020).
38. Agawin, N. S. R., Ferriol, P., Sintes, E. & Moyà, G. Temporal and spatial variability of in situ nitrogen fixation activities associated with the Mediterranean seagrass *Posidonia oceanica* meadows. *Limnol. Oceanogr.* **62**, 2575–2592 (2017).
39. Lepoint, G., Millet, S., Dauby, P., Gobert, S. & Bouquegneau, J. M. Annual nitrogen budget of the seagrass *Posidonia oceanica* as determined by in situ uptake experiments. *Mar. Ecol. Prog. Ser.* **237**, 87–96 (2002).
40. Salk, K. R., Erler, D. V., Eyre, B. D., Carlson-Perret, N. & Ostrom, N. E. Unexpectedly high degree of anammox and DNRA in seagrass sediments: Description and application of a revised isotope pairing technique. *Geochim. Cosmochim. Acta* **211**, 64–78 (2017).
41. Touchette, B. W. & Burkholder, J. A. M. Review of nitrogen and phosphorus metabolism in seagrasses. *J. Exp. Mar. Biol. Ecol.* **250**, 133–167 (2000).
42. Dang, H., Li, T., Chen, M. & Huang, G. Cross-ocean distribution of Rhodobacterales bacteria as primary surface colonizers in temperate coastal marine waters. *Appl. Environ. Microbiol.* **74**, 52–60 (2008).
43. Mejia, A. Y. et al. Assessing the ecological status of seagrasses using morphology, biochemical descriptors and microbial community analyses. A study in *Halophila stipulacea* (Forsk.) Aschers meadows in the northern Red Sea. *Ecol. Indic.* **60**, 1150–1163 (2016).
44. Trevathan-Tackett, S. M. et al. Spatial variation of bacterial and fungal communities of estuarine seagrass leaf microbiomes. *Aquat. Microb. Ecol.* **84**, 59–74 (2020).
45. Matallana-Surget, S. et al. Proteogenomic Analysis of Epibacterium Mobile BBCC367, a Relevant Marine Bacterium Isolated From the South Pacific Ocean. *Front. Microbiol.* **9**, 3125 (2018).
46. Durham, B. P. et al. Draft genome sequence of marine alphaproteobacterial strain HIMB11, the first cultivated representative of a unique lineage within the Roseobacter clade possessing an unusually small genome. *Stand. Genom. Sci.* **9**, 632–645 (2014).
47. Li, Y. et al. Microbiota and functional analyses of nitrogen-fixing bacteria in root-knot nematode parasitism of plants. *Microbiome* **11**, 1–23 (2023).
48. Lesser, M. P., Morrow, K. M., Pankey, S. M. & Noonan, S. H. C. Diazotroph diversity and nitrogen fixation in the coral *Stylophora pistillata* from the Great Barrier Reef. *ISME J.* **12**, 813–824 (2018).
49. Moynihan, M. A. et al. Coral-associated nitrogen fixation rates and diazotrophic diversity on a nutrient-replete equatorial reef. *ISME J.* **16**, 233–246 (2022).
50. Lindström, K. & Mousavi, S. A. Minireview Effectiveness of nitrogen fixation in rhizobia. *Micro. Biotechnol.* **13**, 1314–1335 (2020).

51. Avis, T. J., Gravel, V., Antoun, H. & Tweddell, R. J. Multifaceted beneficial effects of rhizosphere microorganisms on plant health and productivity. *Soil Biol. Biochem* **40**, 1733–1740 (2008).
52. Blanchet, E. et al. Quorum sensing and quorum quenching in the Mediterranean Seagrass *Posidonia Oceanica* microbiota. *Front. Mar. Sci.* **4**, 218 (2017).
53. Bergman, B., Sandh, G., Lin, S., Larsson, J. & Carpenter, E. J. *Trichodesmium* – a widespread marine cyanobacterium with unusual nitrogen fixation properties. *FEMS Microbiol. Rev.* **37**, 286–302 (2013).
54. Berrendero, E. et al. Nitrogen fixation in a non-heterocystous cyanobacterial mat from a mountain river. *Sci. Rep.* **6**, 30920 (2016).
55. Crump, B. C., Wojahn, J. M., Tomas, F. & Mueller, R. S. Metatranscriptomics and amplicon sequencing reveal mutualisms in seagrass microbiomes. *Front. Microbiol.* <https://doi.org/10.3389/fmicb.2018.00388> (2018).
56. Weigel, B. L., Miranda, K. K., Fogarty, E. C., Watson, A. R. & Pfister, C. A. Functional Insights into the Kelp Microbiome from Metagenome-Assembled Genomes. *mSystems* **7**, e0142221 (2022).
57. Sanders-Smith, R. et al. Host-Specificity and Core Taxa of Seagrass Leaf Microbiome Identified Across Tissue Age and Geographical Regions. *Front. Ecol. Evol.* **8**, 1–13 (2020).
58. Zhang, Z. et al. Long-Term Survival of *Synechococcus* and Heterotrophic Bacteria without External Nutrient Supply after Changes in Their Relationship from Antagonism to Mutualism. *mBio* **12**, e0161421 (2021).
59. Van Duc, L. et al. High growth potential and nitrogen removal performance of marine anammox bacteria in shrimp-aquaculture sediment. *Chemosphere* **196**, 69–77 (2018).
60. Yin, S., Li, J., Dong, H. & Qiang, Z. Unraveling the nitrogen removal properties and microbial characterization of “*Candidatus Scalindua*”-dominated consortia treating seawater-based wastewater. *Sci. Total Environ.* **786**, 147470 (2021).
61. Bondoso, J. et al. Epiphytic Planctomycetes communities associated with three main groups of macroalgae. *FEMS Microbiol. Ecol.* **93**, fiw255 (2017).
62. Lage, O. M., Bondoso, J., Luis, R., Comolli, L. & Bengtsson, M. Planctomycetes and macroalgae, a striking association. *Front. Microbiol.* <https://doi.org/10.3389/fmicb.2014.00267> (2014).
63. Delmont, T. O. et al. Nitrogen-fixing populations of Planctomycetes and Proteobacteria are abundant in surface ocean metagenomes. *Nat. Microbiol.* **3**, 804–813 (2018).
64. Strous, M. et al. Missing lithotroph identified as new planctomycete. *Lett. Nat.* **400**, 446–449 (1999).
65. Jetten, M. S. M. et al. Biochemistry and molecular biology of anammox bacteria. *Crit. Rev. Biochem. Mol. Biol.* **44**, 65–84 (2009).
66. Rambo, I. M., Dombrowski, N., Constant, L., Erdner, D. & Baker, B. J. Metabolic relationships of uncultured bacteria associated with the microalgae *Gambierdiscus*. *Environ. Microbiol.* **22**, 1764–1783 (2020).
67. Hutchins, D. A. & Capone, D. G. The marine nitrogen cycle: new developments and global change. *Nat. Rev. Microbiol.* **20**, 401–414 (2022).
68. Jung, M.-Y. et al. Ammonia-oxidizing archaea possess a wide range of cellular ammonia affinities. *ISME* **16**, 272–283 (2022).
69. Martens-Habbena, W., Berube, P. M., Urakawa, H., De La Torre, J. R. & Stahl, D. A. Ammonia oxidation kinetics determine niche separation of nitrifying Archaea and Bacteria. *Nat. Lett.* **461**, 976–981 (2009).
70. Liu, J., Weinbauer, M. G., Maier, C., Dai, M. & Gattuso, J. P. Effect of ocean acidification on microbial diversity and on microbe-driven biogeochemistry and ecosystem functioning. *Aquat. Microb. Ecol.* **61**, 291–305 (2010).
71. Kroeker, K. J. et al. Impacts of ocean acidification on marine organisms: quantifying sensitivities and interaction with warming. *Glob. Chang Biol.* **19**, 1884–1896 (2013).
72. Kitidis, V. et al. Impact of ocean acidification on benthic and water column ammonia oxidation. *Geophys. Res. Lett.* **38**, L21603 (2011).
73. Fulweiler, R. W., Emery, H. E., Heiss, E. M. & Berounsky, V. M. Assessing the Role of pH in Determining Water Column Nitrification Rates in a Coastal System. *Estuaries Coasts* **34**, 1095–1102 (2011).
74. Apostolaki, E. T., Vizzini, S. & Karakassis, I. Leaf vs. epiphyte nitrogen uptake in a nutrient enriched Mediterranean seagrass (*Posidonia oceanica*) meadow. *Aquat. Bot.* **96**, 58–62 (2012).
75. Ravaglioli, C. et al. Nutrient Loading Fosters Seagrass Productivity Under Ocean Acidification. *Sci. Rep.* **7**, 13732 (2017).
76. Banister, R. B., Schwarz, M. T., Fine, M., Ritchie, K. B. & Muller, E. M. Instability and Stasis Among the Microbiome of Seagrass Leaves, Roots and Rhizomes, and Nearby Sediments Within a Natural pH Gradient. *Microb. Ecol.* <https://doi.org/10.1007/s00248-021-01867-9> (2021).
77. Rotini, A., Conte, C., Winters, G., Vasquez, M. I. & Migliore, L. Undisturbed *Posidonia oceanica* meadows maintain the epiphytic bacterial community in different environments. *Environ. Sci. Pollut. Res.* **30**, 95464–95474 (2023).
78. Lidbury, I., Johnson, V., Hall-Spencer, J. M., Munn, C. B. & Cunliffe, M. Community-level response of coastal microbial biofilms to ocean acidification in a natural carbon dioxide vent ecosystem. *Mar. Pollut. Bull.* <https://doi.org/10.1016/j.marpolbul.2012.02.011> (2012).
79. Cardini, U., Van Hoytema, N., Bednarz, V. N., Al-Rshaidat, M. M. D. & Wild, C. N₂ fixation and primary productivity in a red sea *Halophila stipulacea* meadow exposed to seasonality. *Limnol. Oceanogr.* **63**, 786–798 (2018).
80. Hall-Spencer, J. M. et al. Volcanic carbon dioxide vents show ecosystem effects of ocean acidification. *Nature* **454**, 96–99 (2008).
81. Foo, S. A., Byrne, M., Ricevuto, E. & Gambi, M. C. The carbon dioxide vents of Ischia, Italy, a natural system to assess impacts of ocean acidification on marine ecosystems: An overview of research and comparisons with other vent systems. *Oceanogr. Mar. Biol.* **56**, 237–310 (2018).
82. Basili, M. et al. Major Role of Surrounding Environment in Shaping Biofilm Community Composition on Marine Plastic Debris. *Front. Mar. Sci.* **7**, 262 (2020).
83. Walters, W. et al. Improved Bacterial 16S rRNA Gene (V4 and V4-5) and Fungal Internal Transcribed Spacer Marker Gene Primers for Microbial Community Surveys. *mSystems* **1**, e00009–15 (2016).
84. Martin, M. Cutadapt removes adapter sequences from high-throughput sequencing reads. *EMBnet J.* **17**, 10 (2011).
85. R Core Team. R: A language and environment for statistical computing. R Foundation for Statistical Computing, Vienna, Austria, <https://www.R-project.org> (2021).
86. Callahan, B. J. et al. DADA2: High-resolution sample inference from Illumina amplicon data. *Nat. Methods* **13**, 581–583 (2016).
87. Quast, C. et al. The SILVA ribosomal RNA gene database project: improved data processing and web-based tools. *Nucleic Acids Res.* **41**, D590–D596 (2012).
88. Quinn, T. P., Erb, I., Richardson, M. F. & Crowley, T. M. Understanding sequencing data as compositions: An outlook and review. *Bioinformatics*, <https://doi.org/10.1093/bioinformatics/bty175> (2018).
89. Gloor, G. B., Macklaim, J. M., Pawlowsky-Glahn, V. & Egozcue, J. J. Microbiome Datasets Are Compositional: And This Is Not Optional. *Front. Microbiol.* **8**, 2224 (2017).
90. Oksanen, F. J., et al. Vegan: Community Ecology Package, <https://CRAN.R-project.org/package=vegan> (2020).
91. Anderson, M. J. A new method for non-parametric multivariate analysis of variance. *Austral. Ecol.* **26**, 32–46 (2001).
92. Fernandes, A. D., Macklaim, J. M., Linn, T. G., Reid, G. & Gloor, G. B. ANOVA-Like Differential Expression (ALDEX) Analysis for Mixed Population RNA-Seq. *PLoS One* **8**, e67019 (2013).

93. Nearing, J. T. et al. Microbiome differential abundance methods produce different results across 38 datasets. *Nat. Commun.* **13**, 342 (2022).
94. Klawonn, I. et al. Simple approach for the preparation of 15–15 N 2-enriched water for nitrogen fixation assessments: evaluation, application and recommendations. *Front. Microbiol.* **6**, 769 (2015).
95. Montoya, J. P., Voss, M., Kähler, P. & Capone, D. G. A Simple, High-Precision, High-Sensitivity Tracer Assay for N₂ Fixation. *Appl. Environ. Microbiol.* **62**, 986–993 (1996).
96. Altabet, M. A., Wassenaar, L. I., Douence, C. & Roy, R. A Ti(III) reduction method for one-step conversion of seawater and freshwater nitrate into N₂O for stable isotopic analysis of 15N/14N, 18O/16O and 17O/16O. *Rapid Commun. Mass. Spectrom.* **33**, 1227–1239 (2019).

Acknowledgements

We thank L. Polaková and K. Umbria-Salinas of the SoWa Stable Isotope Facility (České Budějovice, CZ) for their assistance with nitrate isotope measurements. This research was supported by a Ph.D. fellowship co-funded by the Stazione Zoologica Anton Dohrn (SZN) and the University of Bremen (to J.B. and F.P.), a Ph.D. fellowship funded by the Open University – SZN Ph.D. Program (to L.M.M.), and a SZN postdoctoral fellowship (to U.M.). U.C. was partially supported by the Italian PRIN 2022 project ENGAGE (grant n. 20223R4FJK) and PRIN 2022 PNRR project BORIS (grant n. P2022R739J), funded by the European Union – Next Generation EU.

Author contributions

F.P., G.M.Q., U.M., C.W. and U.C. designed the study. F.P., G.M.Q., U.M. and U.C. performed the experiments. J.B., U.M. and T.B.M. performed the mass spectrometry analyses. L.M.M. and G.M.Q. performed the molecular analyses. F.M. and M.A. performed the nutrient analyses. J.B. and L.M.M. analyzed the results. J.B., L.M.M. and U.C. wrote the manuscript with contributions from all co-authors.

Funding

Open Access funding enabled and organized by Projekt DEAL.

Competing interests

The authors declare no competing interests.

Additional information

Supplementary information The online version contains supplementary material available at <https://doi.org/10.1038/s42003-024-06011-0>.

Correspondence and requests for materials should be addressed to Johanna Berlinghof or Ulisse Cardini.

Peer review information *Communications Biology* thanks Khashiff Miranda and the other, anonymous, reviewer(s) for their contribution to the peer review of this work. Primary Handling Editors: Tobias Goris. A peer review file is available.

Reprints and permissions information is available at <http://www.nature.com/reprints>

Publisher's note Springer Nature remains neutral with regard to jurisdictional claims in published maps and institutional affiliations.

Open Access This article is licensed under a Creative Commons Attribution 4.0 International License, which permits use, sharing, adaptation, distribution and reproduction in any medium or format, as long as you give appropriate credit to the original author(s) and the source, provide a link to the Creative Commons licence, and indicate if changes were made. The images or other third party material in this article are included in the article's Creative Commons licence, unless indicated otherwise in a credit line to the material. If material is not included in the article's Creative Commons licence and your intended use is not permitted by statutory regulation or exceeds the permitted use, you will need to obtain permission directly from the copyright holder. To view a copy of this licence, visit <http://creativecommons.org/licenses/by/4.0/>.

© The Author(s) 2024